

Stress analysis of Z - section beam

A. Moharrami

Faculty of Engineering, University of Zanjan, P.O. Box 45195-313, Zanjan, Iran

Abstract. This report is broken down into 5 different sections. The first section outlines the objectives of the experiment conducted and what is hoped to be achieved. The next section summarizes the experimental procedure of the z-beam analysis and gives a detailed description of how different loads were applied to the beam. The next section explains the theoretical principles and the third section describes the software used for the analysis and outlines the different input commands applied within Abaqus and final two sections contain a discussion and conclusion.

[A. Moharrami. **Stress analysis of Z - section beam.** *N Y Sci J* 2019;12(6):78-86]. ISSN 1554-0200 (print); ISSN 2375-723X (online). <http://www.sciencepub.net/newyork>. 10. doi:[10.7537/marsnys120619.10](https://doi.org/10.7537/marsnys120619.10).

Keywords: stress, Z-section, moment, displacement, load.

1. Introduction

Z-section beams are becoming increasingly used in a variety of different engineering applications due to their advantageous mechanical properties. Z-sections are light-weight, resistant to deformation and can handle high shearing stresses. They are commonly used in aircraft structures as wing spars or stringers, in order to resist wing bending and twist, as well as carrying any vertical shearing loads. The aim of this report is to evaluate the mechanical properties of a z-section, both experimentally and theoretically as well as comparing them to software results from Abaqus.

This report is broken down into 5 different sections. The first section outlines the objectives of the experiment conducted and what is hoped to be achieved. The next section summarizes the experimental procedure of the z-beam analysis and gives a detailed description of how different loads were applied to the beam.

The next section explains the theoretical principles behind the mathematical equations used in order to calculate parameters such as shear stress, maximum direct stress, shear flow etc. The equations highlighted in this section were used both for the experimental and theoretical calculations.

The third section describes the software used for the analysis and outlines the different input commands applied within Abaqus to achieve the desired results.

The final two sections contain a discussion and conclusion. The results obtained from the z- beam examination will be evaluated in these sections and any possible sources of error will be scrutinised.

2. Objectives

The main objectives of this experiment are:

- Complete a strain gauge analysis of a z section beam.
- Calculate the direct stress, shear flow and displacement of the beam at varying loads.

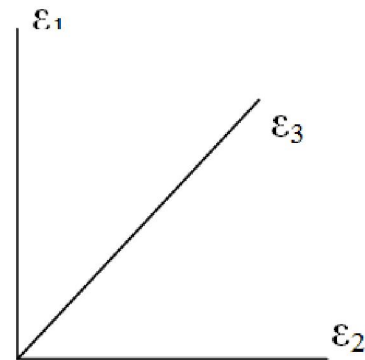
- Complete a theoretical examination of the beam and compare the results to the experiment.
- Construct a Finite Element Analysis of the beam, again compare the results to the theory and experiment.
- Compute the maximum Von Mises stress through FEA.

Construct graphs of the various results

3. Theory

Finding strains

$$\varepsilon_{\theta} = \frac{(\varepsilon_x + \varepsilon_y)}{2} + \frac{(\varepsilon_x - \varepsilon_y)}{2} \cos 2\theta + \frac{\gamma_{xy}}{2} \sin 2\theta$$



$$\varepsilon_a + \varepsilon_b = \varepsilon_2 \quad \dots (1.1)$$

$$\varepsilon_a + \varepsilon_c = \varepsilon_3 \quad \dots (1.2)$$

$$\varepsilon_a - \varepsilon_b = \varepsilon_1 \quad \dots (1.3)$$

Where:

$$\varepsilon_a = \frac{(\varepsilon_x + \varepsilon_y)}{2}$$

$$\varepsilon_b = \frac{(\varepsilon_x - \varepsilon_y)}{2}$$

$$\varepsilon_c = \frac{\gamma_{xy}}{2}$$

Since the strain gauges in this experiment are orientated in the direction of the principal axes, $\varepsilon_2 = \varepsilon_x$ and $\varepsilon_1 = \varepsilon_y$. ε_x and ε_y are changed for calculations depending on the position of the strain rosette on the beam and the orientation of the rosette.

$$\varepsilon_a = \frac{(\varepsilon_2 + \varepsilon_1)}{2} \qquad \gamma_{xy} = 2\varepsilon_3 - \varepsilon_1 - \varepsilon_2 \qquad \dots (1.4)$$

Sub into equation 1.2

$$\sigma_x = \frac{E}{(1 + \nu^2)} (\varepsilon_x + \nu\varepsilon_y) \qquad (2.1)$$

$$\sigma_y = \frac{E}{(1 + \nu^2)} (\varepsilon_y + \nu\varepsilon_x) \qquad (2.2)$$

Now:

$$G = \frac{\tau}{\gamma}$$

$$E = 2G(1 + \nu)$$

Therefore:

$$\tau_{xy} = \frac{E}{2(1 + \nu)} \gamma_{xy} \qquad (2.3)$$

Finding Stress from Strain (Hearn, 1997)

Theoretical Calculations

Shear Flow:

Starting Equation:

$$\frac{dq}{ds} + t \frac{d\sigma_z}{dz} = 0$$

Solving for $\frac{d\sigma_z}{dz}$:

$$\frac{d\sigma_z}{dz} = \left(\frac{SxI_{xx} - SyI_{xy}}{I_{xx}I_{yy} - I_{xy}^2} \right) x - \left(\frac{SyI_{xx} - SxI_{xy}}{I_{xx}I_{yy} - I_{xy}^2} \right) y$$

Substituting for $\frac{dq}{ds}$:

$$\frac{dq}{ds} = - \left(\frac{SxI_{xx} - SyI_{xy}}{I_{xx}I_{yy} - I_{xy}^2} \right) tx - \left(\frac{SyI_{xx} - SxI_{xy}}{I_{xx}I_{yy} - I_{xy}^2} \right) ty$$

Integrating gives:

$$q_s = - \left(\frac{SxI_{xx} - SyI_{xy}}{I_{xx}I_{yy} - I_{xy}^2} \right) \int_0^s tx ds - \left(\frac{SyI_{xx} - SxI_{xy}}{I_{xx}I_{yy} - I_{xy}^2} \right) \int_0^s ty ds$$

For experiment 1; $S_y = 0$

Therefore:

$$q_s = - \left(\frac{SxI_{xx}}{I_{xx}I_{yy} - I_{xy}^2} \right) \int_0^s tx ds - \left(\frac{-SxI_{xy}}{I_{xx}I_{yy} - I_{xy}^2} \right) \int_0^s ty ds$$

This simplifies down to:

$$q_s = \left(\frac{Sx}{I_{xx}I_{yy} - I_{xy}^2} \right) \left(I_{xy} \int_0^s tx ds - I_{yy} \int_0^s ty ds \right)$$

Integrate with respect to s:

$$q_s = \left(\frac{Sx}{I_{xx}I_{yy} - I_{xy}^2} \right) (I_{xy}.t.s.x - I_{yy}.t.s.y)$$

Where for the top flange:

$$X = (-0.07616 + s)$$

$$Y = (0.074405)$$

For the web:

$$X = 0$$

$$Y = (0.074405 + s)$$

For experiment 2, $S_x = 0$:

$$q_s = \left(\frac{Sy}{I_{xx}I_{yy} - I_{xy}^2} \right) \left(I_{xy} \int_0^s tx ds - I_{xx} \int_0^s ty ds \right)$$

For experiment 5 use equation 1.

Direct Stress:

Starting Equation:

$$\sigma = \frac{E}{\rho} (x \sin \alpha + y \cos \alpha)$$

Given:

$$M_x = \int_A \sigma_z y dA$$

$$M_y = \int_A \sigma_z x dA$$

Defining second moments of area:

$$I_{xy} = \int_A xy dA$$

$$I_{yy} = \int_A x^2 dA$$

$$I_{xx} = \int_A y^2 dA$$

Expanding out equation 1:

$$M_x = \frac{E \sin \alpha}{\rho} I_{xy} + \frac{E \cos \alpha}{\rho} I_{xx}$$

$$M_y = \frac{E \sin \alpha}{\rho} I_{yy} + \frac{E \cos \alpha}{\rho} I_{xy}$$

In matrix form:

$$\begin{bmatrix} M_x \\ M_y \end{bmatrix} = \frac{E}{\rho} \begin{bmatrix} I_{xy} & I_{xx} \\ I_{yy} & I_{xy} \end{bmatrix} \begin{bmatrix} \sin \alpha \\ \cos \alpha \end{bmatrix}$$

Which gives:

$$\frac{E}{\rho} \begin{bmatrix} \sin \alpha \\ \cos \alpha \end{bmatrix} = \frac{1}{I_{xx}I_{yy} - I_{xy}^2} \begin{bmatrix} -I_{xy} & I_{xx} \\ I_{yy} & -I_{xy} \end{bmatrix} \begin{bmatrix} M_x \\ M_y \end{bmatrix}$$

The direct stress equation now gives:

$$\sigma_z = \left(\frac{M_x (I_{yy}y - I_{xy}x)}{I_{xx}I_{yy} - I_{xy}^2} \right) + \left(\frac{M_y (I_{xx}x - I_{xy}y)}{I_{xx}I_{yy} - I_{xy}^2} \right) \quad (1)$$

Expanding I_{xy} gives:

$$I_{xy} = \int_A XY dA - b \int_A X dA - a \int_A Y dA + ab \int_a dA$$

If $M_x = 0$,

$$\sigma_z = \left(\frac{M_y (I_{xx}x - I_{xy}y)}{I_{xx}I_{yy} - I_{xy}^2} \right)$$

If $M_y = 0$,

$$\sigma_z = \left(\frac{M_x (I_{yy}y - I_{xy}x)}{I_{xx}I_{yy} - I_{xy}^2} \right)$$

Finding Displacements:

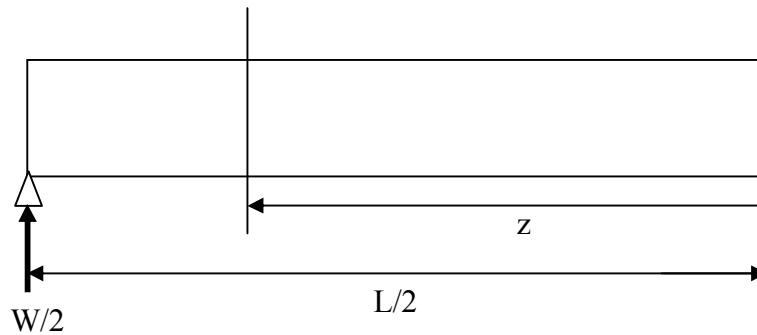
Deflections due to bending relationship:

$$\begin{Bmatrix} \frac{\partial^2 u}{\partial z^2} \\ \frac{\partial^2 v}{\partial z^2} \end{Bmatrix} = \frac{1}{E(I_{xx}I_{yy} - I^2_{xy})} \begin{bmatrix} -I_{xy} & I_{xx} \\ I_{yy} & -I_{xy} \end{bmatrix} \begin{Bmatrix} M_x \\ M_y \end{Bmatrix} \quad (4.1)$$

Expanding 4.1:

$$\frac{\partial^2 u}{\partial z^2} = \frac{-I_{xy}M_x}{E(I_{xx}I_{yy} - I^2_{xy})} + \frac{I_{xx}M_y}{E(I_{xx}I_{yy} - I^2_{xy})} \quad (4.2)$$

Assume vertical load only so that $M_y = 0$



$$M_x = \frac{W}{2} \left(\frac{L}{2} - z \right) \quad (4.3)$$

Replacing M_x in equation 4.2

$$\frac{\partial^2 u}{\partial z^2} = \frac{-I_{xy} \left[\frac{W}{2} \left(\frac{L}{2} - z \right) \right]}{E(I_{xx}I_{yy} - I^2_{xy})}$$

Integrating gives:

$$\frac{\partial u}{\partial z} = \frac{-I_{xy}W}{2E(I_{xx}I_{yy} - I^2_{xy})} \left(\frac{Lz}{2} - \frac{z^2}{2} + A \right) \quad (4.4)$$

A second integration gives:

$$u = \frac{-I_{xy}W}{2E(I_{xx}I_{yy} - I^2_{xy})} \left(\frac{Lz^2}{4} - \frac{z^3}{6} + Az + B \right) \quad (4.5)$$

To determine constants of integration, the following boundary conditions were applied

$$\text{@ } z = 0, \frac{\partial u}{\partial z} = 0$$

$$\text{@ } z = \frac{L}{2}, u = 0$$

Applying the first boundary condition to equation 4.4 gives $A = 0$

Applying the second boundary condition to equation 4.5 gives:

$$B = \frac{-L^3}{24}$$

By substituting this value of B into equation 4.5 and by applying the same integrations to the expanded matrix 4.1, two expressions for displacement in the X and Y directions are found as follows:

$$u = \left[\frac{-I_{xy}W_y}{2E(I_{xx}I_{yy} - I^2_{xy})} + \frac{I_{xx}W_x}{2E(I_{xx}I_{yy} - I^2_{xy})} \right] \left(\frac{Lz^2}{4} - \frac{z^3}{6} - \frac{L^3}{24} \right)$$

$$v = \left[\frac{I_{yy}W_y}{2E(I_{xx}I_{yy} - I^2_{xy})} - \frac{I_{xy}W_x}{2E(I_{xx}I_{yy} - I^2_{xy})} \right] \left(\frac{Lz^2}{4} - \frac{z^3}{6} - \frac{L^3}{24} \right)$$

4. Experimental Procedure

1. The beam was loaded in the X-direction from 0-25kg in increments of 5kg with the displacement sensors monitoring displacement in the X-direction.
2. After each load was applied, strain oscillations were monitored on screen and a reading taken once the oscillations had died down.
3. The beam was then unloaded in the same increments and readings taken after each decrement.
4. Keeping the displacement sensors in the same place, the beam was loaded in the Y-direction from 0-14kg and then up to 44kg in increments of 10kg.
5. The displacement sensors were then moved to measure displacement in the Y-direction and steps 1-4 were repeated.
6. Finally, the displacement sensors were removed and the beam was loaded in both the X and Y directions simultaneously using the following loading sequence.

| | |
|--------------------|-----------------------|
| X Load (kg) | 0 – 5 – 10 – 15 – 20 |
| Y Load (kg) | 0 – 14 – 24 – 34 – 44 |

7. Data from the tests was collected in an Excel sheet and manipulated to obtain stress values from the strain readings.
8. Because the load was applied using levers, the force transmitted to the beam needed to be calculated using moment arms and then converted to Newtons.

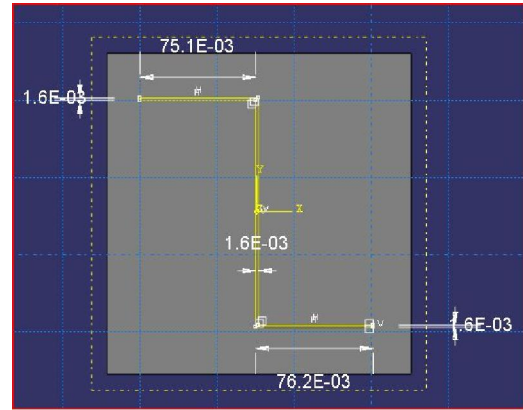


Figure 1. Z-section beam cross section Geometry

5. Finit Element Analysis Geometry of Beam

The Z-section beam in question was measured and the resulting geometries were extrapolated and inserted into Abaqus FEA solver. Geometry was measured with the highest level of accuracy available via measuring tape and utilisation of Vernier calliper.

The Z section sketch shown represents the precise dimensions used in Abaqus for the purpose of analysis. All dimensions in the image are represented in meters and as can be derived from the image:

Thickness = 1.6mm; web height = 148.81mm; top flange width = 751mm; bottom flange width = 76.2mm.

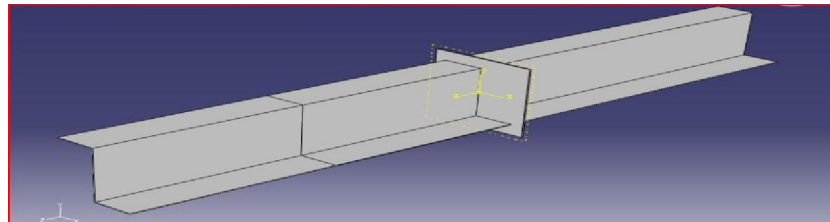


Figure 2. Beam Geometry Isometric view illustration of strain gauge plain

Meshing

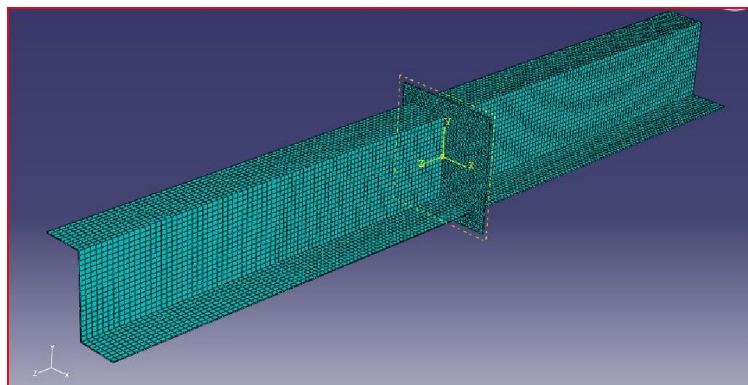


Figure 2. Illustration of seed size and mesh type that was applied to nozzle model

As is also evident from figure, a square plate is located at a location in the vicinity of the middle of the span of the beam. This plate serves the purpose of providing an attachment point for load inputs which will be explained in further detail at a later stage.

Shown above in figure is a pictorial representation of the seed size and meshing type that was used throughout the structure of the Z-section beam. After a lengthily h-refinement process, the results being obtained for the Von Mises stress values balanced out at a global seed size value of 0.008m. Subsequently, 0.008m seed size was used at the area of interest, and an arbitrarily chosen value was used on the centre plate. The element type that was chosen was based on the hexagonal dominated element type with a linear geometric order.

The Hexagonal dominated element shape was chosen due to its large number of degrees of freedom, 6 nodes in each element, each node having three degrees of freedom giving a total of 18 DOF per

element. The primary reason behind choosing a hex-dominated mesh however, was so that a straight line/linear data path could easily be defined along the region where the strain gauges were placed as is seen in figure.

Application of boundary conditions

Each of the two ends of the z-section beam was fixed uniquely on the testing apparatus. These connections were imitated and emulated in Abaqus FEA solver in the form of boundary conditions as follows in figure. Figure illustrates the location of where each boundary condition is applied, and also what type of motion the boundary condition permits or resists. In the following images, the following is described:

U_1 =translation in X direction; U_2 =translation in y direction; U_3 =translation in z direction.

UR_1 =Rotation about X-axis; UR_2 =Rotation about y-axis; UR_3 =Rotation about z-axis.

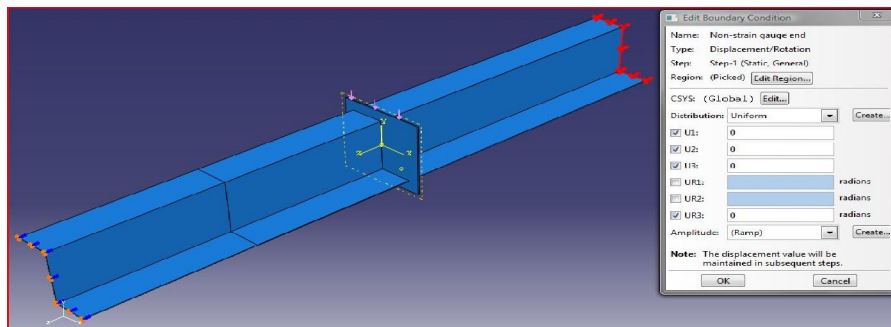


Figure 3. Boundary conditions at the non-strain gauge end

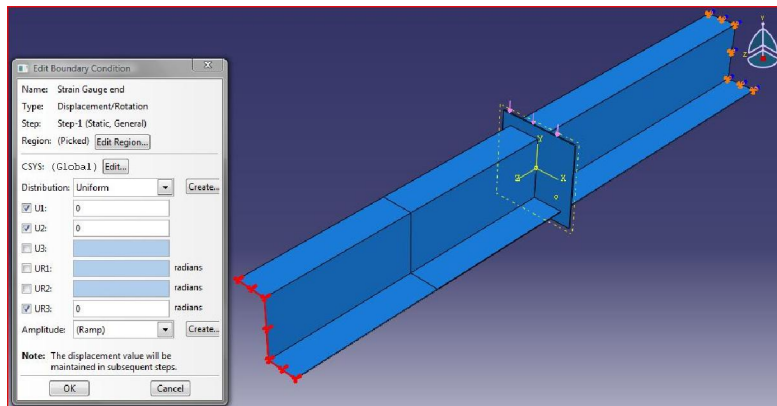


Figure 4. Boundary conditions at the strain gauge end

Applying loads to the model

In application in the experimental segment of this report, it is shown that the load is transmitted to the beam via a pin joint in each corresponding axis on the centre plate. An assumption was made in the FEA portion of the study whereby a continuous uniformly

distributed pressure load was applied in the direction of the load, and it was applied to either the top or side surface of the centre plate.

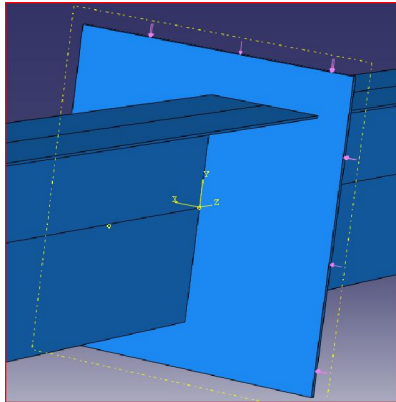
The magnitude of these loads was calculated using the principle that a pressure is force acting over an area. For the purpose of the FEA solver, only the

maximum loads in both the x and y directions were solved for (as is seen in table 1) as it was these loads

that acted as the worst case scenarios and were of most interest for the purpose of analysis.

Table 1. (right) Pressure loads acting upon centre plate in X and Y directions

| | Force (N) | Area (M ³) | Pressure (N/M ³) |
|-------------|-----------|------------------------|------------------------------|
| X-direction | 865.84 | 0.0006 | 1443066.667 |
| Y-direction | 1510.74 | 0.0006 | 2517900 |



combination of both as per laboratory experimentation.

Data acquisition

As previously mentioned, a hex dominated mesh was chosen in order to position a data path across the z-section beam from one flange tip to the other as seen in figure. This data path for all intensive purposes was used as the x-axis datum line for the stress and shear stress calculations. The data path length had been normalised to be represented as a unit length for easier future calculations. XY data in the form of various field outputs were then plotted along the data path in order to produce representative graphs.

Three combinations of loadings were utilised throughout the FEA portion of the analysis, that is, a load was applied in the x direction, y direction, and a

6. Result

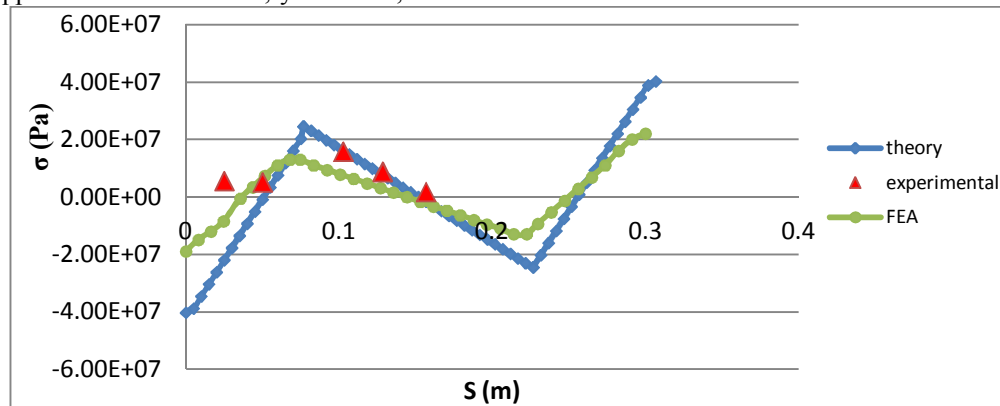


Figure 5: X-load direct Stress

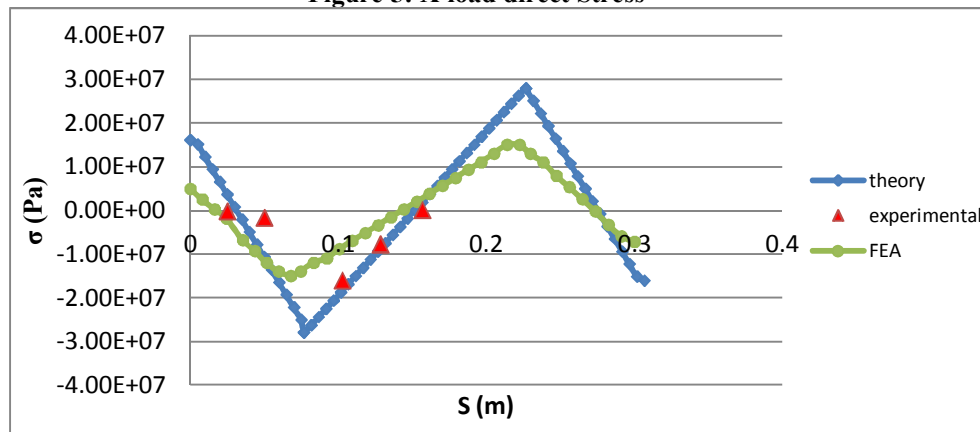


Figure 6: Y-load Direct Stress

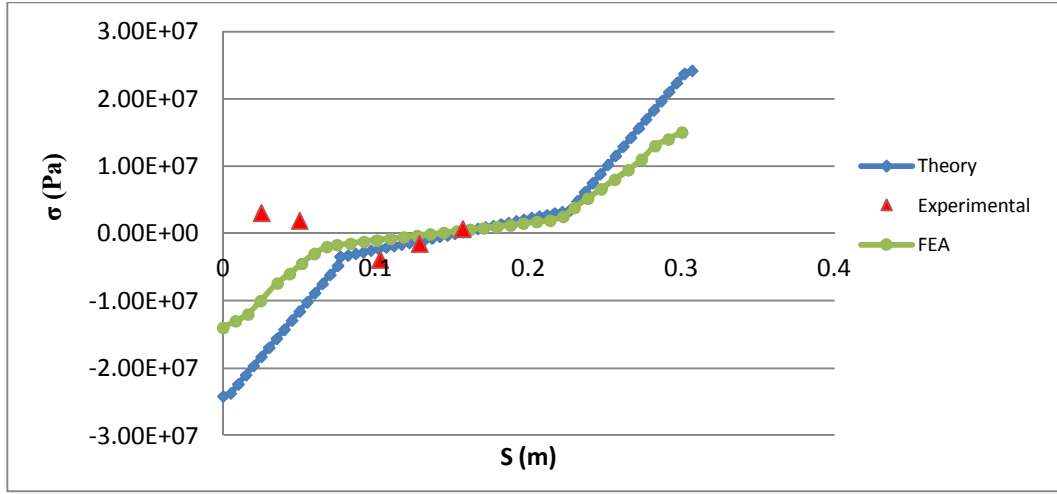


Figure 7: XY-load Direct Stress

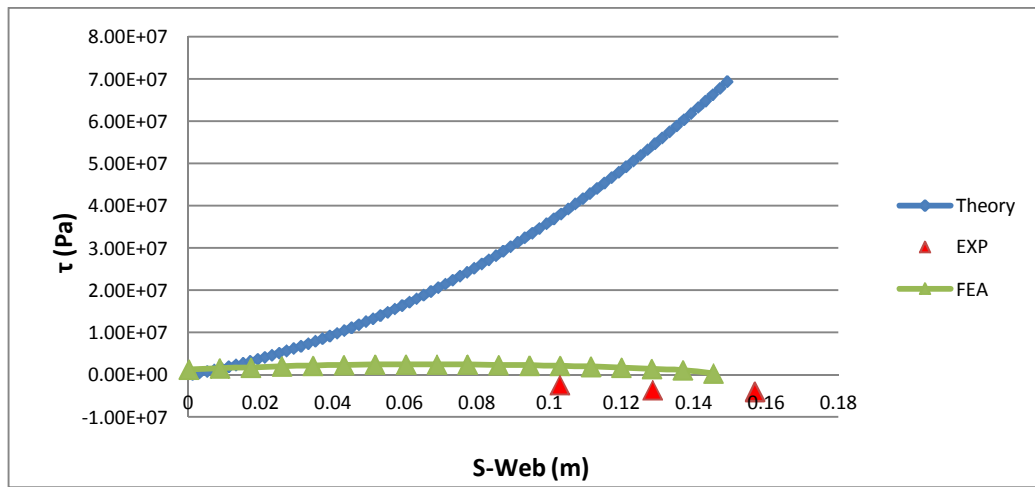
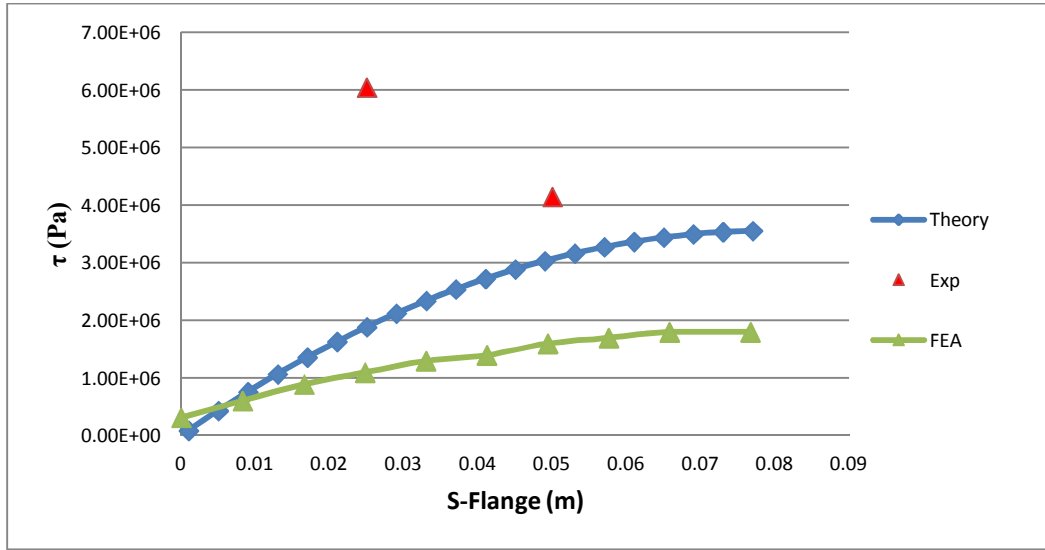


Figure 9 & 10: x-Shear on top flange and Web

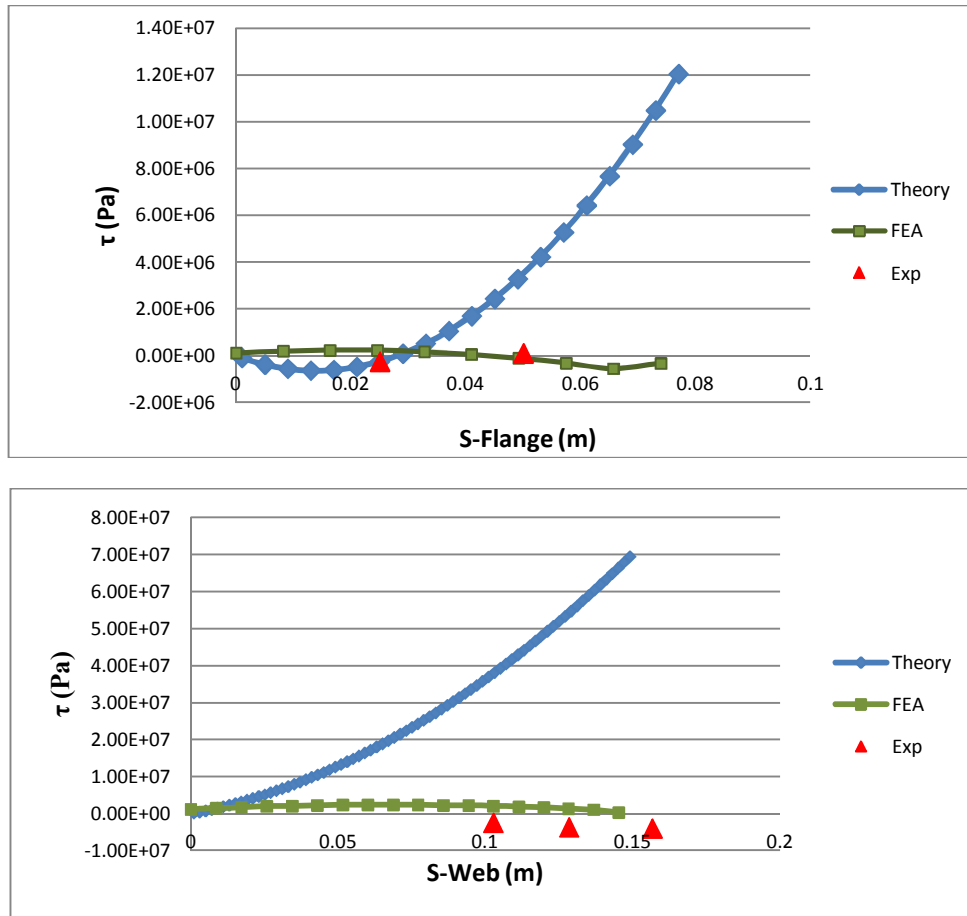


Figure 11 & 12: Y-Shear on top flange and Web

7. Discussion & Conclusion

As previously mentioned all the data plotted above corresponds to the maximum loading in each configuration. As seen above in Figures 15,16 and 17 the bending stress data for the numerical, theoretical and experimental calculations is very similar. The stress where the web meets the flange is noted to be high and also the stress on the neutral axis is zero which is to be expected. From the data collected for 'Test 2' it can be seen that the stresses at the outer edge of the flange are higher experimentally than predicted theoretically and numerically. This can be put down to the fact that during the test warping was noted at the point of loading. This could have led to an uneven stress distribution at the strain gauge locations.

For the displacement data it can be seen that although the numerical and theoretical data coincide,

the experimental data is somewhat greater. This can be seen in Figures 18,19,20 and 21. This could be down to the fact that over the years the beam may have been loaded beyond its yield strength and plastic deformation may have occurred. It is important to note however that the beam does follow the same trend as the other calculated data.

References

1. Hearn, E. J. (1997) *Mechanics of Materials 1*, 3rd ed., Oxford: Butterworth-Heinemann.
2. Megson, T. H. (2007) *Aircraft Structures for Engineering Students*, 4th ed., Oxford: Butterworth-Heinemann.
3. McCarthy, C. (2009), *ME4227: Aircraft Structures*, 26 Nov, University of Limerick, unpublished.